

Influence of the Electron Charge Distribution on Surface-Plasmon Dispersion

ALAN J. BENNETT

General Electric Research and Development Center, Schenectady, New York 12301

(Received 1 August 1969)

The effects of the spatial variation of the electron density on the surface-plasmon dispersion relation are investigated. We show that measurements of that relation are a useful probe of the electron density in the surface region. Previous calculations on homogeneous materials have predicted a linear or quadratic dependence of the frequency on momentum parallel to the surface. We find that the usual surface-plasmon resonance frequency at first decreases with increasing momentum and then increases with further increases in momentum. This behavior agrees with the experimentally observed dispersion. Additional higher-frequency surface modes, similar to those observed in laboratory plasmas, are identified.

I. INTRODUCTION

THE self-consistent charge density and potential at a metal-vacuum interface have been calculated by various workers.¹⁻⁵ The potential is probed by many experiments,⁶ e.g., field emission, thermionic emission, and photoemission. A practical means of measuring the charge density has, however, not as yet been suggested. We calculate, in this paper, the dependence of the surface-plasmon energy on its momentum parallel to the surface⁷⁻⁹ and show that measurements¹⁰ of that function are a useful probe of the equilibrium electron density.

The important effects of a nonuniform charge density on the plasma oscillations in a laboratory discharge tube are well known. Microwave experiments^{11,12} show that a series of surface-plasma resonance modes are observed rather than the single-surface mode of frequency

$$\omega_{s1} = \omega_p / \sqrt{2}$$

calculated by assuming a uniform equilibrium electron density.¹³ Here the bulk-plasma frequency $\omega_p^2 = 4\pi n_0 e^2 / m$, where $-e$ and m are the electron charge and mass, respectively. n_0 is the constant value of electron density deep in the sample.

The physical origin of the additional resonances has been extensively discussed.¹⁴ It was first assumed that the various resonances were due to the momentum

dependence of the plasma frequency.¹⁵ If the additional plasma waves are ones which propagate through the entire sample, the boundary conditions demand that, in the direction of finite sample extent, the allowed values of the momentum be proportional to $1/L$, where L is the sample dimension. The spacing between the resonances predicted by this approach is, in fact, 10–100 times smaller¹⁴ than observed for modes of frequency less than $\omega_{pm}^2 = 4\pi e^2 n_m / m$, where n_m is the maximum value of the density in the sample. This has been attributed to the nonuniform equilibrium electron density.¹⁶⁻²⁰ In a typical cylindrical plasma column, the density $n(r)$ varies over much of the radius, its maximum value being in the center, i.e., at $r=0$. Plasma waves of frequency ω_s less than ω_{pm} can propagate in the regions of low density near the boundaries but are unable to penetrate the higher-density region. The effective length that determines the allowed values of the momentum in the radial direction is thus much less than the radius and is, in fact, given by the distance between the wall at $r=R$ and the point $r=r_c$, determined by the condition $\omega_s^2 = 4\pi n(r_c) e^2 / m$.

The hydrodynamic theory of the electron gas has been used to investigate the above effects. Hoh¹⁸ qualitatively studied the modes of frequency greater than ω_{s1} in a slab geometry. He ignored the dependence of those modes on their momentum parallel to the interface. Parker, Nickel, and Gould^{19,20} have performed quantitative calculations of ω_{s1} and some higher modes in a cylindrical geometry. The momentum dependence of the resonant frequencies was investigated by including both dipole and quadrupole plasma oscillations.

We wish to consider, in this paper, similar effects present in the longitudinal surface-plasma (plasmon) oscillation of the electron gas in a metal. The existence of the surface-plasmon mode of frequency $\omega_{s1}(k=0)$

¹ J. Bardeen, Phys. Rev. **49**, 653 (1936).

² A. J. Bennett and C. B. Duke, *Proceedings Fourth International Materials Symposium, University of California, Berkeley*, (John Wiley & Sons, Inc., New York, 1969).

³ A. J. Bennett and C. B. Duke, Phys. Rev. (to be published).

⁴ J. R. Smith, Phys. Rev. **181**, 522 (1969).

⁵ N. D. Lang, Solid State Commun. (to be published).

⁶ R. Gomer, *Field Emission and Field Ionization* (Harvard University Press, Cambridge, 1961).

⁷ H. Kanazawa, Progr. Theoret. Phys. (Kyoto) **26**, 851 (1961).

⁸ R. H. Ritchie, Progr. Theoret. Phys. (Kyoto) **29**, 607 (1963).

⁹ H. Raether, in *Springer Tracts in Modern Physics*, edited by G. Höhler (Springer-Verlag, New York, 1965), Vol. 38.

¹⁰ C. Kunz, Z. Physik **196**, 311 (1966).

¹¹ L. Tonks, Phys. Rev. **37**, 1458 (1931); **38**, 1219 (1931).

¹² A. Dattner, Ericsson Tech. **8**, 1 (1963); Phys. Rev. Letters **10**, 205 (1963).

¹³ N. Herlofson, Arkiv Fysik **3**, 247 (1951).

¹⁴ G. Bekefi, *Radiation Processes in Plasmas* (John Wiley & Sons, Inc., New York, 1966).

¹⁵ R. W. Gould, in Linde Conference on Plasma Oscillations, Spencer, Indiana, 1959 (unpublished).

¹⁶ F. W. Crawford, Phys. Letters **5**, 244 (1963).

¹⁷ P. Weissglas, Phys. Rev. Letters **10**, 206 (1963).

¹⁸ F. C. Hoh, Phys. Rev. **133**, A1016 (1964).

¹⁹ J. C. Nickel, J. V. Parker, and R. W. Gould, Phys. Rev. Letters **11**, 183 (1963).

²⁰ J. V. Parker, J. C. Nickel, and R. W. Gould, Phys. Fluids **7**, 1489 (1964).

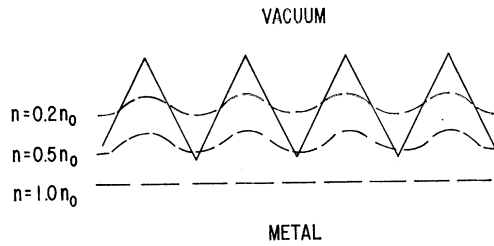


FIG. 1. Schematic drawing of the positive and negative charge densities near a metal-vacuum interface. The solid lines show the boundary of the positive, i.e., ion charge density. The dashed lines represent equidensity curves for the negative, i.e., electron charge density. n_0 is the bulk value of the electron density in the metal.

$=\omega_p/\sqrt{2}$ was first emphasized by Ritchie²¹ and observed by Powell and Swan.^{22,23} The use²⁴ of the ideal plasma dielectric constant and classical electrostatics is sufficient to obtain the above long-wavelength result for the surface-plasmon frequency in a semi-infinite homogeneous medium. Microscopic derivations of this result have been presented by Fedders²⁵ and Feibelman²⁶ who formally included the case of an inhomogeneous medium. The surface plasmon can, of course, propagate parallel to the surface with momentum k . Ritchie,⁸ using a hydrodynamic approach, found that the resonant frequency depended linearly on k for the case of a semi-infinite homogeneous medium. A quantum-mechanical calculation by Kanazawa⁷ indicated a quadratic dependence of the surface-plasmon frequency on wave vector.

Neither of these calculations agrees with the recent high-energy electron transmission measurements of Kunz¹⁰ which indicate an initial decrease in frequency with increasing k followed by an increase when k is increased further.

It is important to differentiate between the k dependence considered here ($0.01 k_F < k < 0.5 k_F$, where $k_F \sim 1 \text{ \AA}^{-1}$ is the Fermi wave vector), and that observed⁹ for $k < k_p = \omega_p/c \approx 0.01 \text{ \AA}^{-1}$ due to the transverse character acquired by the surface-plasmon field.²⁷⁻²⁹

We show that the experimental results of Kunz are a consequence of the inhomogeneous equilibrium electron density. We use a jellium model of a metal in which the positive ions are represented by a smeared out positive background charge. First-principles calculations¹⁻⁵ of the electron charge density at the surface of that model system indicate that the electron density falloff is monotonic and can be roughly represented by a linear relationship.

The simple jellium model used in those calculations fails to represent the actual differences in the self-consistent charge densities and potentials at different single-crystal surfaces of the same material. Different single-crystal surfaces are distinguished by characteristic protrusions of the surface atoms into the vacuum. As first noted by Smoluchowski,³⁰ the kinetic energy of the system is reduced if the electron density is relatively smooth, i.e., it does not follow the contours of the actual positive charge surface. This behavior is schematically shown in Fig. 1. Smoluchowski's model calculations show, in fact, that the electron density has about the same characteristic falloff length on the different faces of a bcc lattice, and, while not completely smooth, does not closely follow the surface contours. The positive-charge contours differ from surface to surface. This causes different electric fields to exist and accounts for the different measured work functions. This situation may, in fact, affect the surface-plasmon frequencies observed on different single-crystal surfaces of the same material. We, therefore, generalize our jellium model to investigate that possibility.

Our use of the hydrodynamic equations for the modified jellium model of a semi-infinite metal is really valid only for wavelengths greater than the interatomic spacing. Large inhomogeneity effects are, in fact, found for such wavelengths and, in addition, the method gives some indication of the proper results even when not strictly valid.

We ignore the damping of the plasma oscillations by their excitation of single electron-hole pairs. In the case of bulk plasmons, this process can occur only for $k > k_c$, where $k_c \sim (\hbar\omega_p/2E_F)k_F$.⁹ In the case of surface plasmons, although the surface serves as a momentum sink, and thus such decay is permitted even for $k < k_c$, the surface-plasmon lifetime is rather long for such wave vectors.³¹

For a fixed bulk density, we calculate numerically the effect of different equilibrium electron distributions on the surface-plasmon dispersion relation. Comparison of the calculated characteristics with actual experimental data provides a measure of the equilibrium charge distribution at the surface. Our analysis when used with Kunz's Mg data indicates a characteristic decay length of about 3 \AA and suggests the desirability of an experimental search for a single higher-energy surface-plasmon mode predicted in that case.

In Sec. II, we exhibit the general hydrodynamic equations and introduce our model of the metal. Section III consists of a presentation of our numerical results and a comparison with experiment.

II. GENERAL EQUATIONS AND MODEL

Our treatment of the surface-plasma modes at a metal-vacuum interface parallels previous work on the

²¹ R. H. Ritchie, Phys. Rev. **106**, 874 (1957).

²² C. J. Powell and J. B. Swan, Phys. Rev. **115**, 869 (1959).

²³ C. J. Powell and J. B. Swan, Phys. Rev. **116**, 81 (1959).

²⁴ E. A. Stern and R. A. Ferrell, Phys. Rev. **120**, 130 (1960).

²⁵ P. A. Fedders, Phys. Rev. **153**, 438 (1967).

²⁶ P. J. Feibelman, Phys. Rev. **176**, 551 (1968).

²⁷ R. A. Ferrell, Phys. Rev. **111**, 1214 (1958).

²⁸ R. H. Ritchie and H. B. Eldridge, Phys. Rev. **126**, 1935 (1962).

²⁹ E. N. Economou, Phys. Rev. **182**, 539 (1969).

³⁰ R. Smoluchowski, Phys. Rev. **60**, 661 (1941).

³¹ R. H. Ritchie and A. L. Marusak, Surface Sci. **4**, 234 (1966).

collective modes in laboratory plasmas, in particular that of Parker, Nickel, and Gould.^{19,20} The continuity equation is give by

$$\partial n / \partial t + \nabla \cdot (n \mathbf{v}) = 0, \quad (2.1)$$

and the force equation by

$$\partial \mathbf{v} / \partial t + (\mathbf{v} \cdot \nabla) \mathbf{v} = (1/mn) [-ne\mathbf{E} - \nabla p]. \quad (2.2)$$

Here $-e$, m , and \mathbf{v} are the electron's charge, mass, and velocity, respectively, n is the electron density, E is the electric field, and p is the pressure. In an actual metal, the fixed positive ion and electron gas mixture constitutes a self-bound system. The binding energy consists¹⁻⁵ of a bulk contribution due to the quantum-mechanical exchange and correlation potentials and a surface contribution due to the Hartree (direct) potential. As a somewhat crude but adequate approximation for the present problem, we have assumed that the first two contributions confine the electron gas to the region $z < 0$. The electric field in that region is given by the Poisson equation

$$\nabla \cdot E = 4\pi(e/\epsilon_0)(N_i - n), \quad (2.3)$$

where N_i is the positive ion density and ϵ_0 is the dielectric constant of free space.

We assume that the quantities which enter the above equations are given by the sum of steady state, i.e., $\mathbf{v}=0$, and nonequilibrium parts

$$\begin{aligned} n &= n_0 f(\mathbf{r}) + n_1(\mathbf{r})e^{-i\omega t}, \\ \mathbf{E} &= \mathbf{E}_0(\mathbf{r}) + \mathbf{E}_1(\mathbf{r})e^{-i\omega t}, \\ p &= p_0(\mathbf{r}) + p_1(\mathbf{r})e^{-i\omega t}, \\ \mathbf{v} &= \mathbf{v}_1(\mathbf{r})e^{-i\omega t}, \end{aligned} \quad (2.4)$$

where n_0 is the constant bulk electron density and

$$\begin{aligned} f(x, y, z \rightarrow -\infty) &= 1, \\ f(x, y, z > 0) &= 0. \end{aligned} \quad (2.5)$$

These definitions when used in Eqs. (2.1)–(2.3) yield the following equations, first order in the perturbation:

$$i\omega n_1 = n_0 \nabla \cdot (f \mathbf{v}_1), \quad (2.6)$$

$$i\omega m n_0 f \mathbf{v}_1 = +en_1 \mathbf{E}_0 + en_0 f \mathbf{E}_1 + \nabla p_1, \quad (2.7)$$

$$\nabla \cdot \mathbf{E}_1 = -(4\pi e/\epsilon_0)n_1, \quad (2.8)$$

where \mathbf{E}_0 is given by the zeroth-order equation

$$\nabla \cdot E_0 = +(4\pi e/\epsilon_0)(N_i - n_0 f). \quad (2.9)$$

We consider only longitudinal plasma oscillation and introduce a scalar potential such that

$$\mathbf{E}_1 = -\nabla \Phi. \quad (2.10)$$

The pressure deviation p_1 is taken as adiabatic

$$p_1 = m\beta^2 n_1, \quad (2.11)$$

where β will be specified in Sec. III.

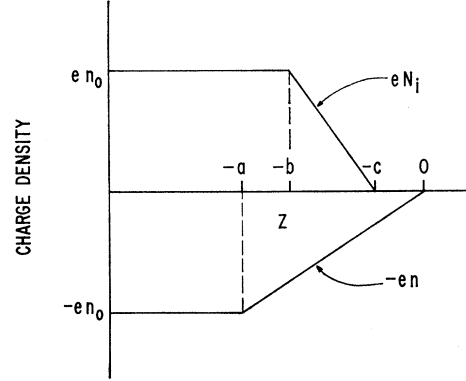


FIG. 2. Positive and negative charge distributions at the one-dimensional model metal-vacuum interface. n is the electron density, N_i is the effective ion density, and n_0 is the bulk density.

As discussed below, we will consider only an essentially one-dimensional model of the metal-surface system. The quantities in Eqs. (2.4) are, therefore, assumed to be of the form

$$g(\mathbf{r}) = g_0(z) + g_1(z)e^{i(k_x x + k_y y)}$$

and Φ is taken as

$$\Phi(\mathbf{r}) = \varphi(z)e^{i(k_x x + k_y y)},$$

where k_x and k_y are components of the wave vector parallel to the junction. Substituting Eq. (2.7) in Eq. (2.6), and letting $\epsilon \equiv eE_0/m\omega_p^2$, we obtain

$$\begin{aligned} \frac{d^4 \varphi}{dz^4} &= \frac{\omega_p^2}{\beta^2} \left\{ -\epsilon \frac{d^3 \varphi}{dz^3} + \left(\frac{2k^2 \beta^2}{\omega_p^2} - \frac{\omega^2}{\omega_p^2} + f - \frac{d\epsilon}{dz} \right) \frac{d^2 \varphi}{dz^2} \right. \\ &\quad \left. + \left(\epsilon k^2 + \frac{df}{dz} \right) \frac{d\varphi}{dz} \right. \\ &\quad \left. + \left[k^2 \left(\frac{\omega^2}{\omega_p^2} - f \right) - \frac{k^4 \beta^2}{\omega_p^2} + k^2 \frac{d\epsilon}{dz} \right] \varphi \right\}, \end{aligned} \quad (2.12)$$

where $k^2 = k_x^2 + k_y^2$. Equation (2.12) is valid in the region $z < 0$. For $z > 0$, Φ satisfies

$$(d^2/dz^2 - k^2)\varphi = 0. \quad (2.13)$$

At the $z=0$ surface, electrostatics demands that φ and $d\varphi/dz$ be continuous. In addition, the electron current across the boundary must also be zero, and hence $v_1(0^-) = 0$. Using Eq. (2.7), we find that this implies

$$d^3 \varphi / dz^3 - k^2 d\varphi / dz|_{z=0} = 0, \quad (2.14)$$

since $E_0(0) = 0$ by charge neutrality and $f(0) = 0$ by definition.

We must now specify ϵ and $d\epsilon/dz$ in the junction region. In order to define a one-dimensional model which preserves the physical information essential to our problem, we recall, from the discussion of Sec. I, that

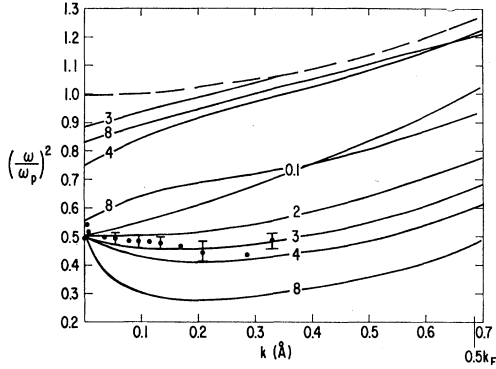


FIG. 3. Square of the surface-plasmon frequency versus k , the momentum parallel to the surface, for a Mg-vacuum interface. E_0 , the steady-state electric field, is set equal to zero. The various curves are labeled by their values of a (\AA), the characteristic electron decay length at the surface. The points and error bars are the experimental data of Kunz (Ref. 10). The dashed curve shows the bulk-plasmon dispersion relation.

the electron distribution at an undisturbed surface has been found to vary strongly only in the z direction. The positive charge distribution at the surface is, however, a function of both the perpendicular and parallel coordinates.

Our approximation, sufficient to estimate roughly the difference in work function at different single-crystal surfaces, consists of using a positive charge distribution which is averaged over x and y and is, thus, a function only of the distance from the surface. As shown in Fig. 2, the equilibrium electron charge density distribution is assumed to be equal to a constant $-en_0$ for $z < -a$ and to decrease linearly to zero in the region $-a < z < 0$. The fixed positive ions are represented by a jellium model of smeared out positive charge. That positive charge density is equal and opposite in sign to the bulk electron density for $z < -b$ and decreases linearly to zero in the region $-b < z < -c$. The quantity ϵ is given by Eq. (2.9) as

$$\begin{aligned} \epsilon &= 0, & z < -a, \\ \epsilon &= +(z+a)^2/2a, & -a < z < -b, \\ \epsilon &= (-cz^2/a - cz - c^2/2)/(a-2c), & -b < z < -c, \\ \epsilon &= z^2/2a, & -c < z < 0. \end{aligned} \quad (2.15)$$

The condition $a-c=b$ is required to ensure charge neutrality.

We conclude this section by comparing the above formulation with previous work. Hoh used the WKB method to study qualitatively the $\omega_s > \omega_p/\sqrt{2}$ surface modes in a slab plasma whose equilibrium electron density decreased linearly to zero at the boundary. He set $E_0=0$ and ignored the k dependence of the resonances and terms of order $(df/dz)/f$. Parker, Nickel, and Gould calculated the dipole and quadrupole surface modes of a cylindrical plasma column. They used the equilibrium electron distribution characteristic

of that system which varies³² for all values of r and found E_0 by assuming a Maxwellian velocity distribution for the electron gas.

III. RESULTS

A. Numerical Results

We now obtain the surface-plasmon resonance frequencies of our metal-vacuum system. Equation (2.12) has four linearly independent solutions. For $z < -a$, where ϵ and $d\epsilon/dz$ are zero, and $f(z)=1$, those solutions can be taken as

$$\begin{aligned} \varphi_1 &= e^{+kz}, & \varphi_2 &= e^{-kz}, \\ \varphi_3 &= e^{+\gamma z}, & \varphi_4 &= e^{-\gamma z}, \end{aligned} \quad (3.1)$$

where

$$\gamma = (\omega_p^2 + \beta^2 k^2 - \omega^2)^{1/2} / \beta. \quad (3.2)$$

The condition $\gamma=0$ yields the bulk plasma frequency. A comparison with a quantum-mechanical calculation³³ of that quantity indicates that for consistency we must take

$$\beta^2 = \frac{2}{5} V_F^2, \quad (3.3)$$

where V_F is the Fermi velocity. We discard the two solutions which are unbounded as $z \rightarrow -\infty$.

The continuations of φ_1 and φ_3 into the region $-a < z < 0$ are obtained by numerically solving Eq. (2.12) using a Runge-Kutta method. The potential in that region is then given by the linear combination

$$\varphi < = A\varphi_1(z) + B\varphi_3(z), \quad (3.4)$$

where A and B are constants to be determined. When $z > 0$, the potential satisfies Eq. (2.13) whose solution, bounded as $z \rightarrow \infty$, is given by

$$\varphi > = C e^{-kz}. \quad (3.5)$$

Equation (2.14) is used to solve for A in terms of B . Continuity of φ and $d\varphi/dz$ at $z=0$ then determines the plasma-resonance frequencies.

The surface-plasmon dispersion relation has been obtained analytically⁸ for a homogeneous system ($a \rightarrow 0$), i.e., one in which (a) $\epsilon=0$ and $d\epsilon/dz=0$ for all z and (b) $f=1$ for $z < 0$ and $f=0$ for $z > 0$. In that limit, our numerical results must agree with the expression

$$\omega_{s1} = \omega_p / \sqrt{2} [1 + (\beta/\sqrt{2}\omega_p)k]. \quad (3.6)$$

For a fixed electron density, we vary the characteristic decay lengths (a and c) and observe the change in the surface-plasmon dependence on momentum. Calculations were performed for electron densities corresponding to both Al and Mg. The general character of the results is very similar in the two cases. We present the Mg ($n_0 = 8.6 \times 10^{22} \text{ e/cm}^3$) curves, since experimental data exist for that material. Figures 3 and 4 show the

³² J. V. Parker, Phys. Fluids **6**, 1657 (1963).

³³ D. Pines, Phys. Rev. **92**, 626 (1953).

square of the reduced surface-plasmon frequency, i.e., $(\omega_s/\omega_p)^2$ versus k for values of $k < 0.5k_F$. In general, the lower-equilibrium density in the surface region results in a lower value for the resonant frequencies. As $k \rightarrow 0$, details of the density distribution near the surface become relatively unimportant and ω_{s1} the usual surface mode, approaches $\omega_p/\sqrt{2}$.

We first consider the case in which the steady-state electric field $E_0(\epsilon)$ is set equal to zero. This corresponds to choosing $c=0$ and represents one limiting case of the type of field behavior possible at a single-crystal surface. The results are shown in Fig. 3. The dispersion curve for $a=0.1 \text{ \AA}$ exhibits the homogeneous material behavior of Eq. (3.6). The curve is monotonically increasing and is fitted very well by Ritchie's result. For somewhat larger values of a , the frequency increases less rapidly with k as illustrated by the $a=2 \text{ \AA}$ result. For larger values of a ($a=3 \text{ \AA}$ and $a=4 \text{ \AA}$), the dispersion curves are no longer monotonic. They first decrease and then increase as k increases. This behavior is accompanied by the appearance of an additional higher-energy surface mode of frequency ω_{s2} , where $\omega_{s1} < \omega_{s2} < \omega_p$. As a is increased still further, the initial decrease in ω_{s1} with increasing k becomes steeper and an additional surface mode appears. The results for $a=8 \text{ \AA}$ ($\omega_{s1}, \omega_{s2}, \omega_{s3}$), when a total of three surface modes are present, are also given in Fig. 3. The frequencies of the higher-energy modes are in rough agreement with Hoh's qualitative calculation.

In order to obtain some measure of the variation in surface-resonant frequencies obtained using different single-crystal surfaces of the same material, we now consider a second limiting case in which $E_0(\epsilon)$ is as large as may be expected. We choose $c=\frac{1}{2}a$ and repeat the above calculations. The results for various values of a are shown in Fig. 4. The frequency of the lowest mode ω_{s1} is somewhat increased compared with that obtained in the first case. As expected, the effect becomes large as a increases. For $a=3 \text{ \AA}$ and $a=4 \text{ \AA}$, the frequencies ω_{s2} of the higher modes are in general affected very little by the presence of the field. However, when $a=8 \text{ \AA}$, the frequency of the highest-energy surface mode ω_{s3} is strongly increased by the field. For $c=4 \text{ \AA}$, in fact, the mode is eliminated.

B. Comparison with Experiment

Kunz¹⁰ has obtained the ω_{s1} -versus- k relationship at an oxide-free polycrystalline Mg surface using a high-energy (34-keV) electron transmission experiment. The solid circles in Figs. 3 and 4 represent a set of his data (the solid circles in Fig. 11 of Ref. 10). The ω_{s1} curve corresponding to $a=3 \text{ \AA}$ best fits the experimental

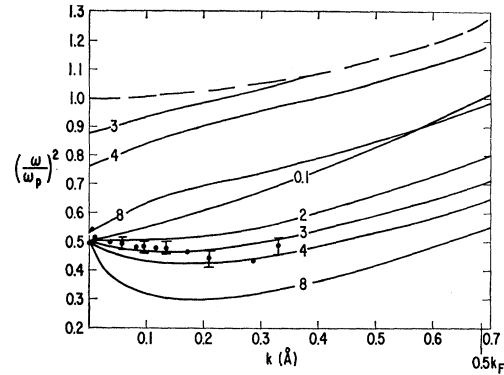


FIG. 4. Square of the surface-plasmon frequency versus k , the momentum parallel to the surface, for a Mg-vacuum interface. E_0 , the steady-state electric field, is that due to a step discontinuity in the positive charge density at the interface. The various curves are labeled by their values of a (\AA), the characteristic electron decay length at the surface. The points and error bars are the experimental data of Kunz (Ref. 10). The dashed curve shows the bulk plasmon dispersion relation.

points. The scatter and relatively large error bars on the experimental points make a more exact fit somewhat difficult. This value for a is in general accord with the Thomas-Fermi screening length of $\sim 0.5 \text{ \AA}$ for Mg and a "first-principles" calculation.⁴ Figures 3 and 4 show that, for $a=3 \text{ \AA}$, a second surface-plasmon mode exists at about $(\omega/\omega_p)^2=0.85$ for $k=0$, and merges with the bulk plasmon frequency at $k \sim 0.4 \text{ \AA}^{-1}$. A successful experimental search for this higher-plasmon branch would help confirm our analysis.

We suggest that measurements of the surface-plasmon dispersion in other polycrystalline materials would provide considerable insight into the variation of the characteristic electron decay length at a surface with density. Since single-crystal sample preparation is difficult, and our calculation of the electric field effects indicates that they are not very large, such experiments on metals are of lower priority. Experimental determination of ω_s versus k for semiconductors in which the characteristic electron decay length a could be very large would be of great interest. The electric field effects may well be important in such cases. The effect of absorbed atoms on the surface-plasmon dispersion should also be measured.³⁴

ACKNOWLEDGMENTS

We wish to thank Dr. R. H. Ritchie for an informative conversation, and Dr. M. J. Rice and Dr. R. E. Kinsinger for critical readings of the manuscript.

³⁴ A. U. MacRae, K. Müller, J. J. Lander, J. Morrison, and J. C. Phillips, Phys. Rev. Letters **22**, 1048 (1969).